Classical cadherins control nucleus and centrosome position and cell polarity

Isabelle Dupin, Emeline Camand, and Sandrine Etienne-Manneville

Institut Pasteur, Cell polarity and migration group, and Centre National de la Recherche Scientifique Unité de Recherche Associée 2582, 75724 Paris, Cedex 15, France

Control of cell polarity is crucial during tissue morphogenesis and renewal, and depends on spatial cues provided by the extracellular environment. Using micropatterned substrates to impose reproducible cell–cell interactions, we show that in the absence of other polarizing cues, cell–cell contacts are the main regulator of nucleus and centrosome positioning, and intracellular polarized organization. In a variety of cell types, including astrocytes, epithelial cells, and endothelial cells, calcium-dependent cadherin-mediated cell–cell interactions induce nucleus and centrosome off-centering toward cell–cell contacts, and promote orientation of the nucleus–centrosome axis toward free cell edges. Nucleus and centrosome off-centering is controlled by N-cadherin through the regulation of cell interactions with the extracellular matrix, whereas the orientation of the nucleus–centrosome axis is determined by the geometry of N-cadherin–mediated contacts. Our results demonstrate that in addition to the specific function of E-cadherin in regulating baso-apical epithelial polarity, classical cadherins control cell polarization in otherwise nonpolarized cells.

Introduction

Regulation of cell polarity and orientation is essential during symmetric and asymmetric cell division and cell differentiation, as well as in a large variety of cellular functions such as T cell interaction with their target cell, synaptic transmission, or cell migration (Krummel and Macara, 2006; Arimura and Kaibuchi, 2007; Etienne-Manneville, 2008). Directed as well as random cell migration is associated with polarization of the cellular machinery in order to define a leading protrusive front and a retracting rear. During cell migration as well as during cell differentiation or polarized cell function, the relative position of the centrosome and the nucleus is generally a good indicator of the orientation of the cell polarity axis (Schliwa et al., 1999; de Anda et al., 2005; Siegrist and Doe, 2006).

Integrin engagement with the extracellular matrix plays a key role in controlling nucleus and centrosome positioning in migrating and immobile cells (Etienne-Manneville and Hall, 2001; Thery et al., 2005, 2006; Peng et al., 2008). In contrast, the role of cell–cell contacts in controlling orientation of the nucleus–centrosome axis remains unclear. Tight junctions are key to the baso-apical polarity of epithelial cells, and are likely to be involved in centrosome apical positioning (Musch, 2004; Shin et al., 2006). Herein, we investigated whether intercellular junctions can promote polarization of nonepithelial cells, such as astrocytes, that do not form tight junctions. We show that anisotropic cell–cell interactions provide extracellular cues that are sufficient to promote cell polarization and orientation toward the free cell edge. In the absence of any other polarizing cues, calcium-dependent classical cadherins, including N-cadherin as well as E-cadherin, control centrosome and nucleus positioning and cell polarization via the regulation of cell interactions with the extracellular matrix and of the actin and microtubule cytoskeletons.

Correspondence to Sandrine Etienne-Manneville: setienne@pasteur.fr

Results and discussion

To examine whether cell–cell contacts could influence intracellular asymmetry, primary rat astrocytes were plated on large (11,000 μm^2) fibronectin-coated circular micropatterns allowing adhesion of five to seven cells (Fig. 1 A). Their migration off the pattern was prevented by treating the glass coverslip with polyethylene glycol. Each astrocyte spread over a large surface compared with other cell types ($\sim$2,000 μm^2), which remained constant in the various conditions used in this study (Table S1). We focused on cells located at the edge of the pattern. These cells have a free edge corresponding to the external limit of the

The Rockefeller University Press $30.00
J. Cell Biol. Vol. 185 No. 5 779–786
www.jcb.org/cgi/doi/10.1083/jcb.200812034

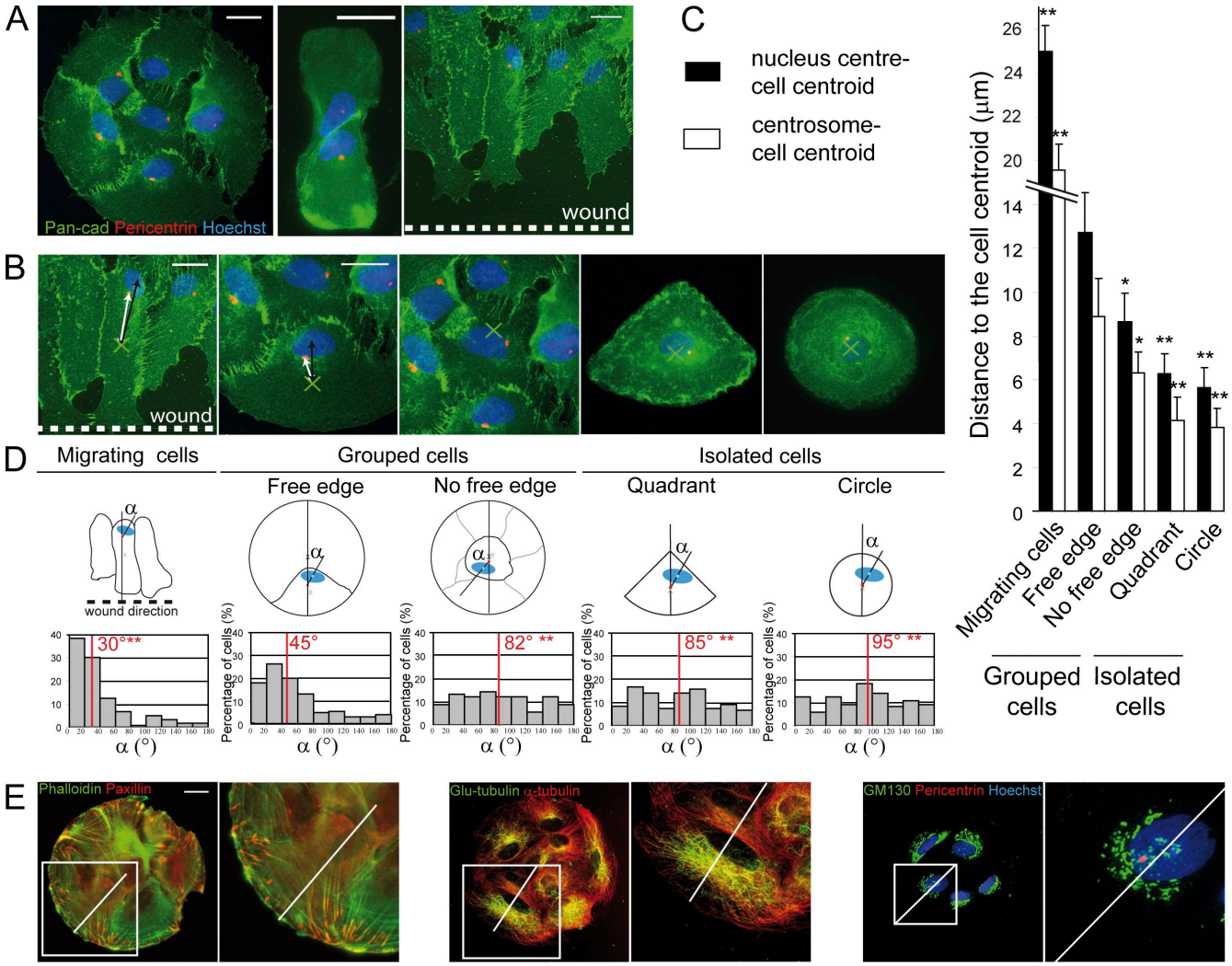

Figure 1. **Cell–cell contacts control intracellular organization and cell orientation.** Primary rat astrocytes were plated onto fibronectin-printed micropatterns or submitted to a wound-healing assay (migrating cells). 7 h later, cells were fixed and stained. (A and B) Pan-cadherin (green), pericentrin (red), and Hoechst (blue) stainings. The green cross indicates the position of the cell centroid, and the arrows show the distance between the cell centroid and the nucleus center (black) or the centrosome (white). (C) Distances between the nucleus and cell centroids (black) and between centrosome and cell centroid (white). (D) Distribution of the angle between the centrosome–nucleus axis and the micropattern radius passing through the centrosome. The median angle is indicated in red. The typical intracellular organization of the cell in each condition is depicted above the distribution graphs (green cross, cell centroid; blue oval, nucleus center; red dot, centrosome). (E, left) Paxillin (red) and phalloidin (green). (middle) α-tubulin (red, for microtubules) and detyrosinated tubulin (green). (right) GM130 (green), pericentrin (red), and Hoechst (blue). Data are given as mean ± SD of three independent experiments totaling at least 120 cells. Statistical differences between grouped cells with a free cell edge and the other conditions are indicated. *, $P < 0.05$; **, $P < 0.005$. Bars, 20 µm.

pattern, and form intercellular junctions with two to three neighboring cells (Fig. 1 A). In these conditions, we observed that the nucleus was off-centered and localized next to cell–cell contacts (Fig. 1, A–C). Nucleus off-centering was also clearly visible in migrating cells of a wound edge (Fig. 1, B–D, migrating cells) as described previously (Gomes et al., 2005). Nucleus recruitment near cell–cell contacts was also visible when two cells interact along a single side (Fig. 1 A, middle). The centrosome was also off-centered in close proximity to the nucleus (Fig. 1, A–C). Accordingly, the distance from the centrosome to the cell centroid (geometric cell center) and the distance from the nucleus to the cell centroid were greatly increased compared with isolated cells in which the centrosome and the nucleus localize near the cell center independently of cell shape (Fig. 1, B and C). To quantify cell orientation, we measured the angle between the nucleus–centrosome axis and a reference radius passing through the centrosome and the micropattern center. This angle can take any value between 0 and 180°, giving a median value of 90° for a population of randomly oriented cells. For a polarized cell oriented toward the free edge of the pattern or toward the wound, this angle is 0° (see diagram in Fig. 1 D). In cells involved in intercellular interactions, the distribution of angles was shifted toward low values (median angle, 45°), which indicates a preferential positioning of the centrosome in front of the nucleus in the direction of the free cell edge (Fig. 1 D). In contrast, in isolated cells, the median angle was close to 90°, which indicates that, in these cells, the centrosome–nucleus axis was randomly oriented (Fig. 1 D). Similarly, cells entirely surrounded by cellular interactions at the

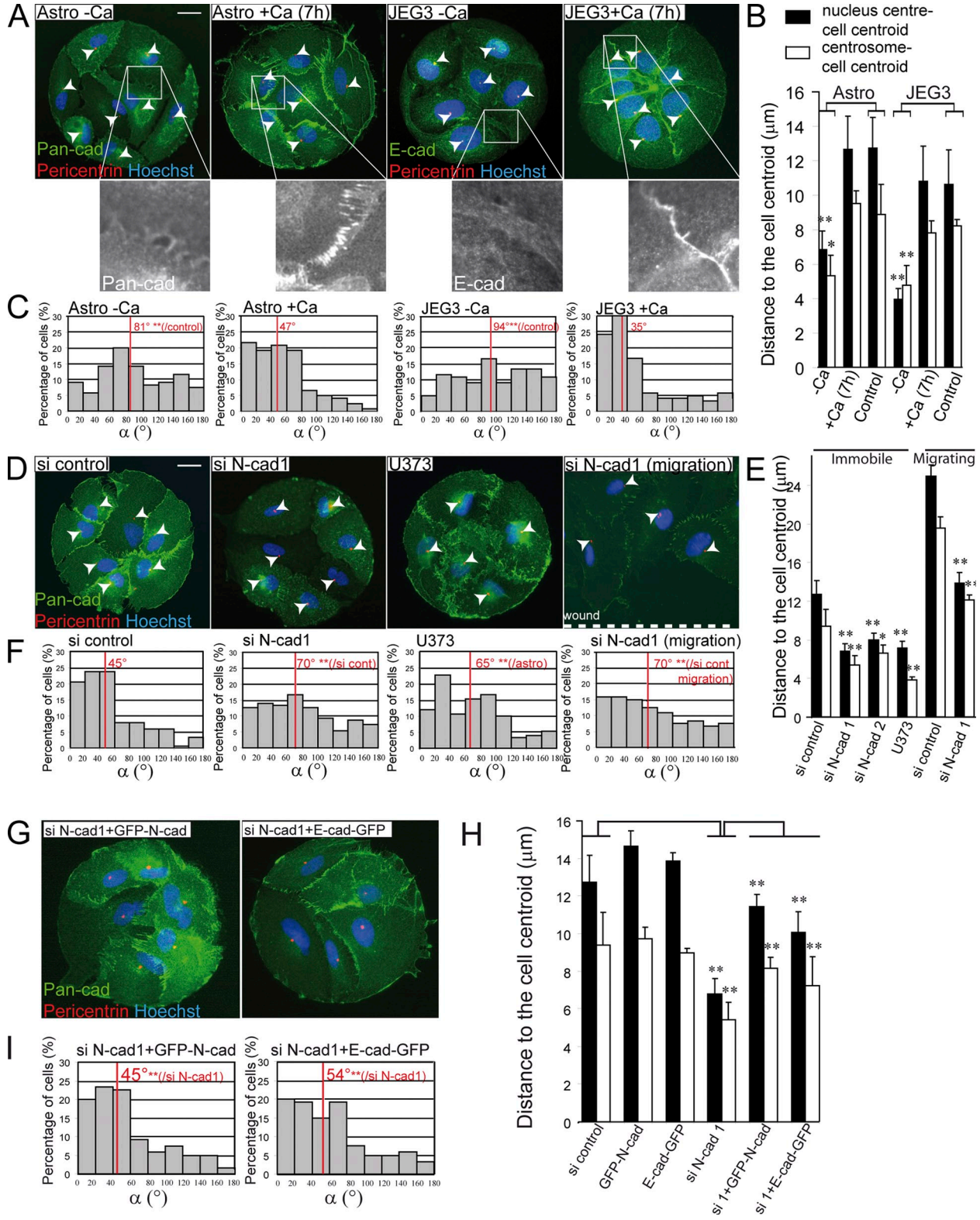

Figure 2. **Classical cadherin-mediated adherens junctions regulate nucleus and centrosome positioning and cell orientation.** (A–C) Astrocytes or JEG3 epithelial cells were plated onto fibronectin-printed micropatterns in the presence of 1.8 mM calcium. Cells were incubated for 2 h in presence of calcium and then for 5 h in calcium-free medium (−Ca), or incubated for 2 h in the absence of calcium and then for 5 h in calcium-containing medium (+Ca). (D–I) 3 d after nucleofection of the indicated siRNAs and pEGFP constructs, astrocytes and U373 astrocytoma cells were either plated onto fibronectin-printed micropatterns (immobile cells) or submitted to a wound-healing assay (migrating cells). (A, D, and G, top) Pan-cadherin or E-cadherin (green), pericentrin (red, white arrowhead), and Hoechst (blue) stainings. (A, bottom) Higher magnification of cadherin staining at cell–cell contacts. Bars, 20 µm. (B, E, and H) Distances between the nucleus and cell centroids (black) and between the centrosome and cell centroid (white). Data are given as mean ± SD of three independent experiments totaling at least 120 cells. (C, F, and I) Distribution of the angle between the centrosome–nucleus axis and the micropattern radius passing through the centrosome. The median angle is indicated in red. Statistical differences are indicated. *, $P < 0.05$; **, $P < 0.005$.

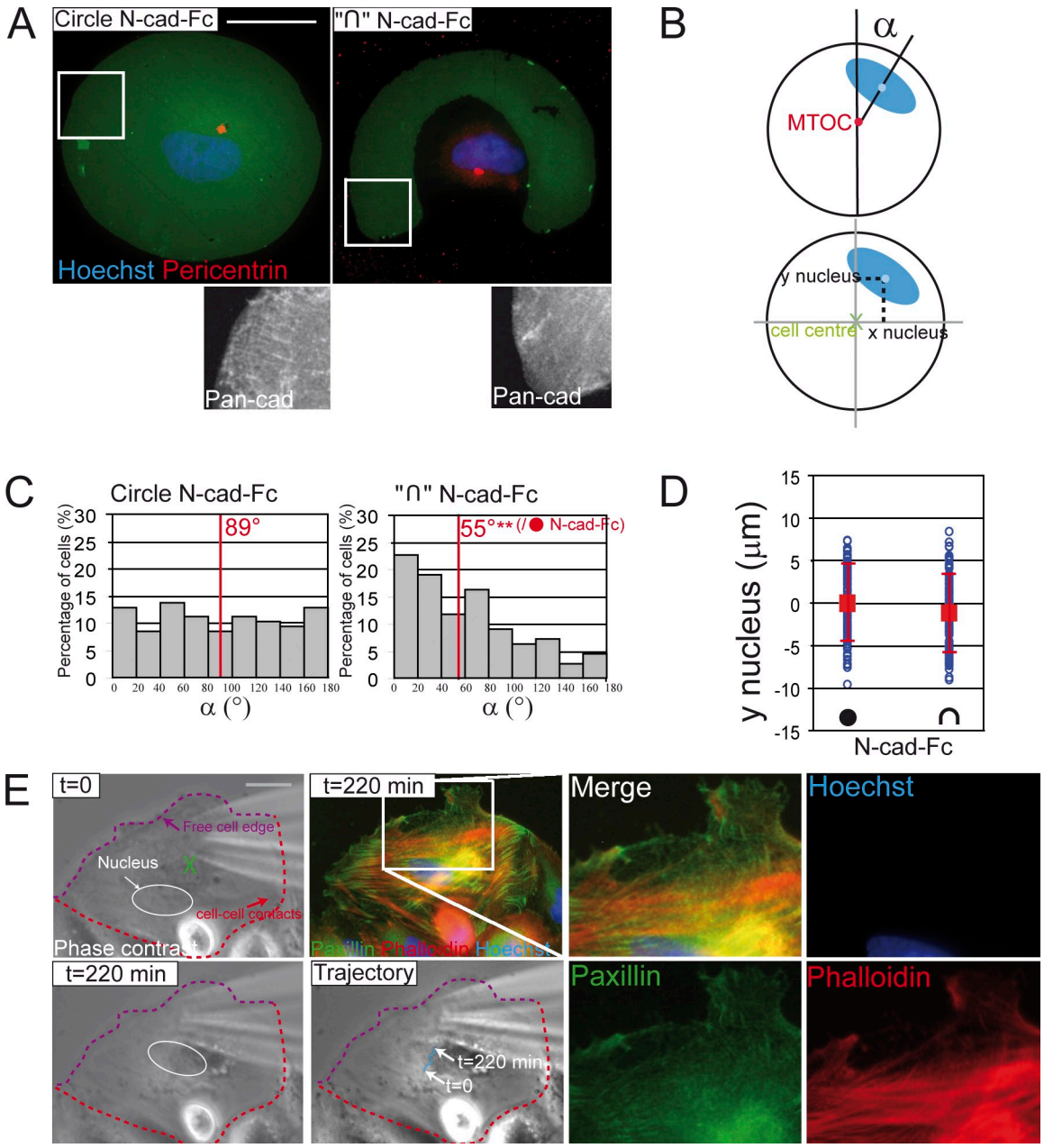

Figure 3. **Asymmetric N-cadherin–mediated interactions are sufficient to promote nucleus–centrosome axis orientation but not nucleus off-centering.** (A–D) Primary rat astrocytes were plated on circle- or ∩-shaped micropatterns coated with N-cadherin–Fc. (A) Pericentrin (red), pan-cadherin (white, and insets below), and Hoechst (blue) stainings. Dextran fluorescence (green) shows the micropattern. Bar, 10 µm. (B) Schematics defining the two measured parameters: the angle "α" (in degrees) between the centrosome–nucleus axis and the micropattern radius passing through the centrosome (red dot), and the distance "y nucleus" (in micrometers) between nucleus (blue dot) and cell (green cross) centers along the symmetry axis (y axis) of the pattern. (C) Angle distribution from at least 110 cells. Median angles and statistical differences are indicated in red. (D) Y nucleus position (blue circles). The red square and bar show mean values ± SD. (E) Astrocytes were plated on large fibronectin micropatterns, and actin was locally disrupted. Selected phase contrast images were taken from Video 2: t = 0, t = 220 min, and the trajectory followed by the nucleus. The cell center (green cross), the nucleus border (white oval), cell–cell contacts (red broken line), and the free cell edge (purple broken line) are shown. At t = 220 min, cells were fixed and stained with anti-paxillin (green), phalloidin (red), and Hoechst (blue). Right panels show a higher magnification image (indicated by the boxed regions) of the contact-free cell edge under the cytochalasin D flow (5 µM) emanating from a micropipette. Bar, 10 µm.

center of large patterns were randomly oriented (Fig. 1, B–D). Cell polarization was also reflected by a polarized intracellular organization. Focal adhesions localize almost exclusively at the free edge, and actin fibers elongate from these focal adhesions toward the cell center (Fig. 1 E, left). The microtubule network extends in the direction of the free edge, with detyrosinated microtubules, the centrosome, and the Golgi apparatus all locating between the nucleus and the free edge (Fig. 1 E, middle and right). These results demonstrate that the anisotropy of cell–cell contacts controls intracellular organization, nucleus and centrosome positioning, and cell orientation in the direction of the free cell edge.

Calcium-free medium rapidly perturbed cell–cell contacts and led to a loss of adherens junctions (compare Fig. 2 A with Fig. 1 B). Concomitantly, the nucleus moved away from the cell

edge toward the cell centroid (Video 1). 3 h after calcium depletion, the intracellular organization was similar to that of isolated cells (Fig. 2, A–C, Astro −Ca). Conversely, calcium addition induced nucleus and centrosome migration toward the newly formed intercellular contacts, and promoted cell orientation toward the free edge (Fig. 2, A–C, +Ca). These results indicate that formation of calcium-dependent cellular interactions promotes nucleus and centrosome movement across the cytoplasm and cell orientation.

Astrocytes form both N-cadherin–mediated adherens junctions and gap junctions (Bennett et al., 2003; Perego et al., 2002). In contrast to epithelial cells, they do not express E-cadherin and do not form tight junctions in mammals (Penes et al., 2005; Mack and Wolburg, 2006). Decrease of N-cadherin expression (80%; Fig. S1 A) after nucleofection with two distinct siRNAs dramatically affected centrosome and nucleus positioning as well as cell orientation in micropatterned plated immobile cells as well as in migrating cells (Fig. 2, D–F). In U373 astrocytoma cells that express low levels of N-cadherin (unpublished data), centrosome and nucleus also localized near the cell center and showed a random orientation, which suggested that loss of cadherins in tumor cells may dramatically perturb cell polarity (Fig. 2, D–F). Cotransfection of an siRNA-resistant mouse N-cadherin or of E-cadherin rescued the phenotype of N-cadherin–depleted astrocytes (Fig. 2, G–I). In JEG-3 epithelial cells that express E-cadherin but not N-cadherin, centrosome and nucleus were located near cell–cell contacts, and cells were oriented toward the free cell edge in a calcium-dependent manner (Fig. 2, A–C). In a similar experiment, endothelial HUVEC cells, which express VE-cadherin, also displayed a polarized phenotype (unpublished data). Together with the recent observation that dominant-negative E-cadherin inhibits cell–cell contact-induced cell orientation (Desai et al., 2009), our results show that calcium-dependent cadherin-mediated adherens junctions control nucleus and centrosome positioning and cell orientation. Moreover, they strongly suggest that in addition to the well-described role of E-cadherin in baso-apical polarity (Nejsum and Nelson, 2007), classical cadherins may play a general function in the control of polarity in a variety of cell types.

We then plated single cells on micropatterns coated with N-cadherin–Fc to mimic cadherin-based cell–cell interactions (Fig. 3, A–D) and test whether asymmetric cadherin-mediated interactions were sufficient to promote cell polarization. On circular N-cadherin–Fc–coated micropatterns, both nucleus and centrosome localized near the cell center, and the orientation of the nucleus–centrosome axis was random (Fig. 3, C and D). When cells were plated on "∩"-shaped N-cadherin–coated micropatterns, the nucleus and centrosome remained near the cell center, but the nucleus–centrosome axis became preferentially oriented toward the nonadhesive cell edge (Fig. 3, C and D). These results show that the geometry of N-cadherin–mediated interactions controls the orientation of the centrosome–nucleus axis but is not sufficient to promote nucleus and centrosome off-centering.

Anisotropic intercellular interactions induce an asymmetric distribution of focal adhesions (Fig. 1 E, left; and Fig. S1 B). Calcium and N-cadherin depletion induce a redistribution of focal adhesions around the entire cell periphery (Fig. S1 B), which indicates that adherens junctions act upstream of integrins to restrict the localization of focal adhesion to the free cell edge. When isolated astrocytes were plated on fibronectin-coated asymmetric micropatterns (Fig. S1, C–E), the nucleus was off-centered and preferentially localized near the nonadhesive region of the cells, showing that anisotropic cell interactions with the extracellular matrix promote nucleus off-centering. We used a micropipette to locally deliver the actin-depolymerizing drug cytochalasin D at the free edge of cells engaged in anisotropic cell–cell contacts. This treatment resulted in local actin depolymerization and focal adhesion disruption (Fig. 3 E), and induced nuclear movement from cell–cell contacts toward the cell center (Fig. 3 E and Video 2). Altogether, these observations strongly suggest that asymmetric N-cadherin–mediated cellular interactions induce nucleus movement toward cell–cell contacts by controlling the localization of cell interactions with the extracellular matrix and the actin cytoskeleton.

Inhibition of calcium-dependent N-cadherin–mediated cell interactions had a strong effect on the organization the microtubule and actin cytoskeletons (Figs. S1 B and S2 A). We asked whether these cytoskeletal elements were involved in the cell–cell contact-controlled nucleus and centrosome positioning. Cell treatment with nocodazole or taxol to disrupt microtubules (Fig. 4, A and B, Noco; and unpublished data) did not affect centrosome off-centering. In contrast, cell treatment with cytochalasin D (Fig. 4, A and B, Cyto D) abolished nucleus off-centering, and also prevented centrosome off-centering (Fig. 4, A and B, CytoD), as expected from the micropipette experiment (Fig. 3 E). Because nucleus and centrosome positioning were similarly affected by actin disruption, we tested the role of the nucleus in centrosome off-centering by enucleating astrocytes. In cells without nucleus, the centrosome localized to the cell center as in isolated cells (Fig. 4, D and E), pointing to an essential role of the nucleus in centrosome positioning near cell–cell contacts.

We then investigated the mechanisms controlling the orientation of the nucleus–centrosome axis. Orientation of the nucleus–centrosome axis was not significantly affected by actin disruption (Fig. 4, A–C), confirming that nucleus and centrosome off-centering and orientation of the nucleus-centrosome axis are controlled by distinct mechanisms. Microtubule disruption by nocodazole or taxol treatment did not strongly perturb the orientation of the nucleus–centrosome axis (Fig. 4 C). This could simply be caused by a steric hindrance of centrosome movement around the nucleus because of the very close proximity of the nucleus to cell–cell junctions. Cells were thus treated with cytochalasin D to displace the nucleus and the centrosome away from cell–cell junctions toward the cell center (Fig. 4 B). In these conditions, the orientation of the nucleus–centrosome axis was severely perturbed by nocodazole treatment (Fig. 4, A–C, CytoD + Noco). Further evidence for a role of microtubules in the orientation of the nucleus–centrosome axis comes from the observations that alteration of the microtubule network leads to an increased distance between the centrosome and the nucleus center (Fig. S2, C and D), and to a perturbation of the preferential orientation of the centrosome relatively to the nucleus axis (Fig. S2 E), which suggests that microtubules contribute to the nucleus–centrosome connection.

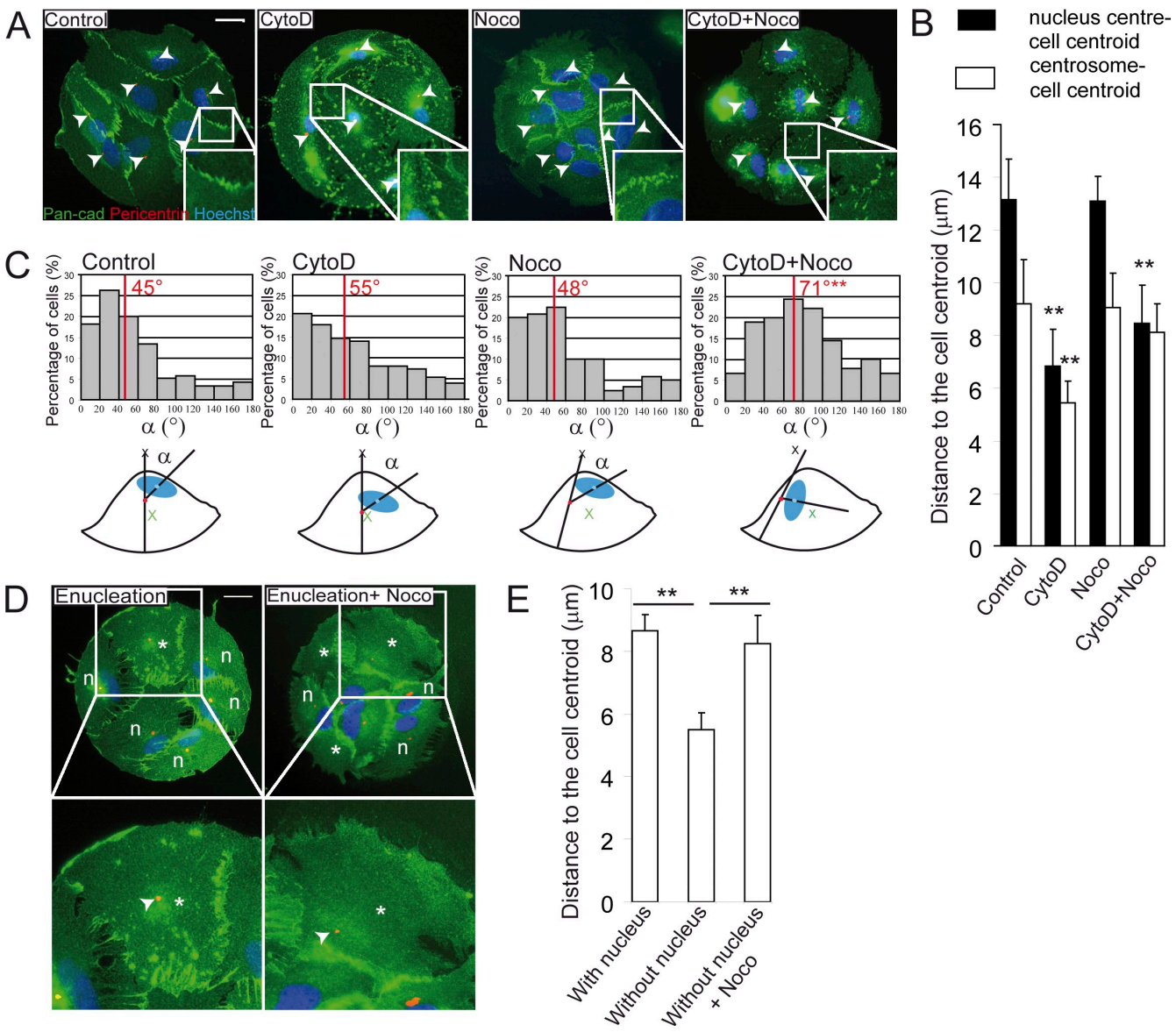

Figure 4. **Actin and nucleus-dependent forces control centrosome positioning.** (A–D) Astrocytes were plated onto fibronectin-printed micropatterns. After 4 h, cells were treated with 1 µM cytochalasin D (CytoD), 20 µM nocodazole (Noco), both (CytoD + Noco), or were enucleated and incubated in the presence (Enucleation + Noco) or absence of nocodazole (Enucleation) for another 3 h. (A) Pan-cadherin (green), pericentrin (red, white arrowhead), and Hoechst (blue) stainings. (insets) Higher magnification images of cadherin staining at cell–cell contacts. Bar, 20 µm. (B) Distances between the nucleus and cell centroids (black) and between centrosome and cell centroid (white). Data are given as mean ± SD of three independent experiments and a total of at least 120 cells. (C) Histograms showing the distribution of angles formed by the centrosome–nucleus axis and the micropattern radius passing through the centrosome. The median angle is indicated in red. Statistical differences between control and inhibitor-treated cells are indicated. Schematics depict the typical intracellular organization in each condition. (D) Pan-cadherin (green), anti-pericentrin (red, white arrowhead), and Hoechst (blue) stainings. Enucleated cells are indicated by an asterisk and nonenucleated cells are indicated by "n". Bottom panels show higher magnification images of an enucleated cell. (E) Distance between the centrosome and the cell centroid in enucleated ("without nucleus") and nonenucleated cells ("with nucleus"). Data are given as mean ± SD of three independent experiments, with a total of at least 100 cells. *, $P < 0.05$; **, $P < 0.005$.

Furthermore, when cells were enucleated, treatment with nocodazole abolished centrosome centering. The centrosome was randomly localized as a consequence; the mean distance between the centrosome and the cell centroid increased (Fig. 4, D and E). We conclude that in absence of the nucleus, microtubule-dependent forces are exerted on the centrosome to position it at the cell center. It is tempting to speculate that, in cells engaged in intercellular interactions, actin-dependent forces exerted on the nucleus bring the nucleus and the centrosome toward cell–cell contacts, whereas microtubule-dependent forces exerted on the centrosome contribute to its positioning in front of the nucleus in the direction of the cell center (Fig. 5).

We show here that classical cadherins, including N-cadherin as well as E-cadherin, control intracellular organization, nucleus and centrosome positioning, and cell orientation in various cell types. In the absence of other polarizing cues that may have a strong effect on microtubule functions, anisotropic cell–cell contacts dictate the orientation of intracellular polarity toward contact-free cell edges. This observation is particularly relevant at tissue borders where contacts between cells expressing different types

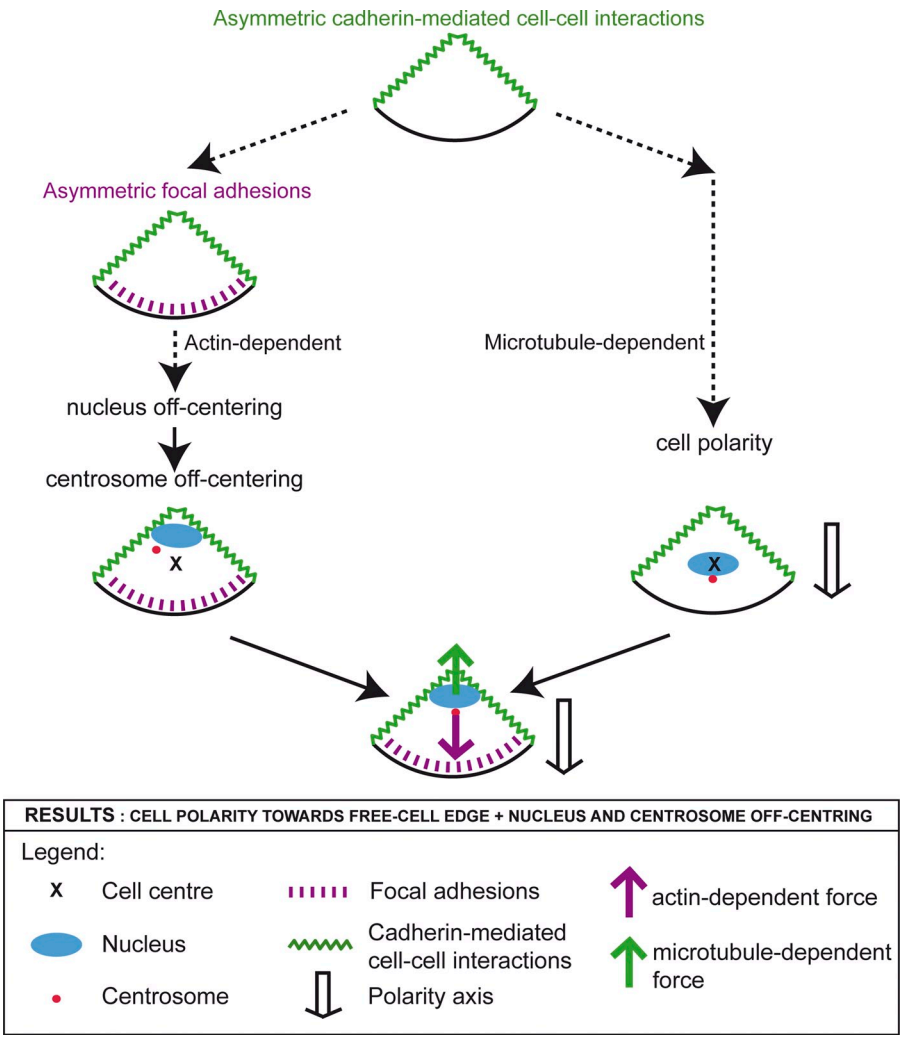

Figure 5. **Model showing the mechanisms involved in nucleus and centrosome positioning and cell orientation in response to anisotropic cell–cell contacts.** Asymmetric cadherin-mediated cell–cell interactions regulate interactions with the extracellular matrix (focal adhesions), and thereby control actin-dependent nucleus and centrosome positioning. Cadherins also control orientation of the nucleus–centrosome axis via a microtubule-dependent pathway.

and levels of cadherins occur. It is also tempting to speculate that regulation of nucleus and centrosome localization by cell–cell contacts may control neuronal polarity in postmitotic differentiating neurons (de Anda et al., 2005). Furthermore, loss of cadherin is frequently associated with the development of highly invasive tumors (Vleminckx et al., 1991; Perego et al., 2002). Our findings suggest that loss of cadherin-mediated adherens junctions may directly contribute to the disruption of cell polarity and lead to the formation of a disorganized tissue due to a random orientation of cell division and cell migration.

Materials and methods

Materials

We used the following reagents: anti–α-tubulin (AbD Serotec); anti-Pan-cadherin CH-19 (Sigma-Aldrich); anti–N-cadherin, anti–β-catenin, anti-GM130, and anti-paxillin (all from BD); anti–E-cadherin (Santa Cruz Biotechnology, Inc.); anti-pericentrin (Covance); anti-microtubule Glu (AbCys); goat anti–human IgG Fcγ, Cy2, Cy5, and TRITC secondary antibodies (Jackson ImmunoResearch Laboratories); pEGFP–N-cadherin (C. Gauthier-Rouviere, Centre de Recherche de Biochimie Macromoléculaire, Montpellier, France; Mary et al., 2002); pEGFP–E-cadherin (P. Cossart, Institut Pasteur, Paris, France; Lecuit et al., 2000); pN-cadherin–Fc (R.M. Mege, Institut du Fer à Moulin, Paris, France; Lambert et al., 2000); cytochalasin D, taxol, and nocodazole (Sigma-Aldrich); Alexa Fluor 488 Phalloidin (Invitrogen); and cRGD (Interchim). siRNA duplexes corresponding to rat N-cadherin starting at nt 677 and 1,734 (available under GenBank/EMBL/DDBJ accession no. AB017695) were obtained from Sigma-Aldrich. siRNA and pEGFP constructs were introduced into cells using nucleofection technology (Amaxa Biosystems; Etienne-Manneville et al., 2005). Purification of the N-cadherin–Fc chimera (extracellular domain of the chicken N-cadherin fused to the human IgG2b Fcγ fragment) was performed as described previously (Lambert et al., 2000).

Stamp fabrication, microcontact printing, and cell plating

Molds for stamps were obtained from Biotray (École Normale Supérieure de Lyon). Stamp fabrication and microcontact printing were performed as described previously (Fink et al., 2007). Briefly, polydimethylsiloxane stamps were coated with fibronectin (0.005%) or with goat anti–human IgG Fcγ (50 μg/ml) for fibronectin or N-cadherin–Fc patterns, respectively. After printing, glass coverslips were then treated with poly-lysine-ethylen glycol to avoid cell spreading outside of the patterns. For the N-cadherin–Fc patterns, coverslips were then incubated overnight at 4°C with a concentration of 5–10 μg/cm^2 of purified N-cadherin–Fc chimera (Lambert et al., 2000). For plating on N-cadherin–Fc micropatterns, cells were treated with 200 μM cRGD to avoid any integrin activation. Culture of primary astrocytes has been described previously (Etienne-Manneville and Hall, 2001; Etienne-Manneville, 2006). U373 astrocytoma cells were grown in minimum essential medium supplemented with 10% fetal calf serum and nonessential amino acids. JEG-3 epithelial cells were grown in minimum essential medium supplemented with 10% fetal calf serum, glutamax, nonessential amino acids, and sodium pyruvate. HUVEC cells were grown in CS-C medium (Sigma Aldrich) supplemented with 10% fetal calf serum, EGF, and endothelial cell attachment factor (Sigma-Aldrich). Cells were trypsinized and agitated for 30 min at 37°C in 0.5% fetal calf serum–containing medium, then deposited on the printed coverslip and centrifuged at 800 rpm for 5 min. For calcium switching, the medium was changed 2 h after centrifugation for calcium-depleted medium (Invitrogen) supplemented with 0.5% fetal calf serum. After 2 h, calcium was

added back in the medium at a final concentration of 1.8 mM. Cell enucleation was performed 4 h after cell plating on micropatterns as described previously (Piel et al., 2000).

Image acquisition and analysis, statistical analysis

Fixed cells were imaged on a microscope (DM6000B; Leica) using an HCX Plan-Apochromat 40×/1.25 oil CS or HCX Plan-Apochromat 63×/1.40 oil CS objective lens (Leica). For time-lapse microscopy, astrocytes were imaged at 37°C with an N Plan 10×/0.25 dry (for Video 1) or a HI Plan CY 40×/0.55 dry (for Video 2) objective lens (Leica) on a microscope (DMI6000B). Imaging medium was either calcium-depleted medium (for Video 1) or classical cultured medium (for Video 2). Microscopes were equipped with a camera (DFC350 FX; Leica), and images were collected with LAS software (Leica). Image analysis and measurements were performed with the ImageJ software (National Institutes of Health; http://rsb.info.nih.gov/ij/). For figures, brightness and contrast were adjusted. Image analysis was always performed on unmodified images. For recording nucleus, centrosome, and pattern centroid positions, a threshold value of fluorescence intensity was chosen to respectively select nucleus, centrosome, or pattern from the appropriate images. The cell contour was manually determined using images of cadherin staining. The coordinates of the centroid of thresholded or selected objects was measured. The distances from the nucleus centroid or the centrosome to the cell centroid were calculated. For grouped cells located at the edge of the pattern, cell orientation was analyzed by measuring the angle between the centrosome–nucleus axis and the centrosome–pattern center radius. For single cells plated on a ∩ shape, cell orientation was analyzed by measuring the angle between the nucleus–centrosome axis and the symmetry axis of the shape. For migrating cells, cell orientation was analyzed by measuring the angle between the centrosome–nucleus axis and an axis perpendicular to the wound. For a polarized cell oriented toward the free edge of the pattern (grouped cells), toward the nonadhesive region of the pattern (∩ shape), or toward the wound (migrating cells), this angle is 0° (see diagrams in Figs. 1 D and 3 B). For a randomly oriented cell, this angle can take any value between 0 and 180°, giving a median value of 90° for a population of randomly oriented cells. Statistical differences were determined using the *t* test for distances comparison and the Wilcoxon test for angles distribution comparison. Statistical significance was defined as $P < 0.05$. To determine the position of the centrosome relative to the nucleus, the thresholded nucleus was fitted by an ellipse. The position of the centrosome relative to this ellipse was then measured.

Online supplemental material

Fig. S1 depicts nucleus positioning promoted by asymmetric cell–matrix interactions, and shows that cadherins control cell–matrix interaction localization. Fig. S2 shows the precise role of microtubules in the cell polarity. Videos 1 and 2 show nucleus migration induced by calcium depletion and local actin depolymerization at the free cell edge, respectively. Table S1 shows the mean spreading area of cells under different conditions. Online supplemental material is available at http://www.jcb.org/cgi/content/full/jcb.200812034/DC1.

We are particularly grateful to Matthieu Piel and René-Marc Mège for their technical support and very helpful discussions. We also thank Pascale Cossart, Cécile Gauthier-Rouvière, Robert Kypta, Paul Lazarrow, Alan Hall, Jean-Baptiste Manneville, and Pierre Vallois for plasmids, scientific discussions, helpful comments on the manuscript, and help with the statistical analyses.

I. Dupin is funded by the Ministère de la Recherche, and E. Camand is funded by Association pour la recherche contre le Cancer and the Schlumberger foundation. This work was supported by the Centre National de la Recherche Scientifique (grant 53/0281), the Institut Pasteur, the Fondation de France (grant 200510057), the Institut pour la Recherche sur la Moelle épinière et l'Encéphale, Agence Nationale de la Recherche (grant 032312), and La Ligue contre le Cancer (grant RS 07/75-31). S. Etienne-Manneville is a member of the European Molecular Biology Organization Young Investors Program.

Submitted: 5 December 2008
Accepted: 1 May 2009

References

Arimura, N., and K. Kaibuchi. 2007. Neuronal polarity: from extracellular signals to intracellular mechanisms. *Nat. Rev. Neurosci.* 8:194–205.

Bennett, M.V., J.E. Contreras, F.F. Bukauskas, and J.C. Saez. 2003. New roles for astrocytes: gap junction hemichannels have something to communicate. *Trends Neurosci.* 26:610–617.

de Anda, F.C., G. Pollarolo, J.S. Da Silva, P.G. Camoletto, F. Feiguin, and C.G. Dotti. 2005. Centrosome localization determines neuronal polarity. *Nature.* 436:704–708.

Desai, R.A., L. Gao, S. Raghavan, W.F. Liu, and C.S. Chen. 2009. Cell polarity triggered by cell-cell adhesion via E-cadherin. *J. Cell Sci.* 122:905–911.

Etienne-Manneville, S. 2006. In vitro assay of primary astrocyte migration as a tool to study Rho GTPase function in cell polarization. *Methods Enzymol.* 406:565–578.

Etienne-Manneville, S. 2008. Polarity proteins in glial cell functions. *Curr. Opin. Neurobiol.* 18:488–494.

Etienne-Manneville, S., and A. Hall. 2001. Integrin-mediated Cdc42 activation controls cell polarity in migrating astrocytes through PKCz. *Cell.* 106:489–498.

Etienne-Manneville, S., J.B. Manneville, S. Nicholls, M. Ferenczi, and A. Hall. 2005. Cdc42 and Par6-PKCz regulate the spatially localized association of Dlg1 and APC to control cell polarization. *J. Cell Biol.* 170:895–901.

Fink, J., M. Thery, A. Azioune, R. Dupont, F. Chatelain, M. Bornens, and M. Piel. 2007. Comparative study and improvement of current cell micropatterning techniques. *Lab Chip.* 7:672–680.

Gomes, E.R., S. Jani, and G.G. Gundersen. 2005. Nuclear movement regulated by Cdc42, MRCK, myosin, and actin flow establishes MTOC polarization in migrating cells. *Cell.* 121:451–463.

Krummel, M.F., and I. Macara. 2006. Maintenance and modulation of T cell polarity. *Nat. Immunol.* 7:1143–1149.

Lambert, M., F. Padilla, and R.M. Mege. 2000. Immobilized dimers of N-cadherin-Fc chimera mimic cadherin-mediated cell contact formation: contribution of both outside-in and inside-out signals. *J. Cell Sci.* 113:2207–2219.

Lecuit, M., R. Hurme, J. Pizarro-Cerda, H. Ohayon, B. Geiger, and P. Cossart. 2000. A role for alpha-and beta-catenins in bacterial uptake. *Proc. Natl. Acad. Sci. USA.* 97:10008–10013.

Mack, A.F., and H. Wolburg. 2006. Growing axons in fish optic nerve are accompanied by astrocytes interconnected by tight junctions. *Brain Res.* 1103:25–31.

Mary, S., S. Charrasse, M. Meriane, F. Comunale, P. Travo, A. Blangy, and C. Gauthier-Rouviere. 2002. Biogenesis of N-cadherin-dependent cell-cell contacts in living fibroblasts is a microtubule-dependent kinesin-driven mechanism. *Mol. Biol. Cell.* 13:285–301.

Musch, A. 2004. Microtubule organization and function in epithelial cells. *Traffic.* 5:1–9.

Nejsum, L.N., and W.J. Nelson. 2007. A molecular mechanism directly linking E-cadherin adhesion to initiation of epithelial cell surface polarity. *J. Cell Biol.* 178:323–335.

Penes, M.C., X. Li, and J.I. Nagy. 2005. Expression of zonula occludens-1 (ZO-1) and the transcription factor ZO-1-associated nucleic acid-binding protein (ZONAB)-MsY3 in glial cells and colocalization at oligodendrocyte and astrocyte gap junctions in mouse brain. *Eur. J. Neurosci.* 22:404–418.

Peng, H., W. Shah, P. Holland, and S. Carbonetto. 2008. Integrins and dystroglycan regulate astrocyte wound healing: the integrin beta1 subunit is necessary for process extension and orienting the microtubular network. *Dev. Neurobiol.* 68:559–574.

Perego, C., C. Vanoni, S. Massari, A. Raimondi, S. Pola, M.G. Cattaneo, M. Francolini, L.M. Vicentini, and G. Pietrini. 2002. Invasive behaviour of glioblastoma cell lines is associated with altered organisation of the cadherin-catenin adhesion system. *J. Cell Sci.* 115:3331–3340.

Piel, M., P. Meyer, A. Khodjakov, C.L. Rieder, and M. Bornens. 2000. The respective contributions of the mother and daughter centrioles to centrosome activity and behavior in vertebrate cells. *J. Cell Biol.* 149:317–330.

Schliwa, M., U. Euteneuer, R. Graf, and M. Ueda. 1999. Centrosomes, microtubules and cell migration. *Biochem. Soc. Symp.* 65:223–231.

Shin, K., V.C. Fogg, and B. Margolis. 2006. Tight junctions and cell polarity. *Annu. Rev. Cell Dev. Biol.* 22:207–235.

Siegrist, S.E., and C.Q. Doe. 2006. Extrinsic cues orient the cell division axis in *Drosophila* embryonic neuroblasts. *Development.* 133:529–536.

Thery, M., V. Racine, A. Pepin, M. Piel, Y. Chen, J.B. Sibarita, and M. Bornens. 2005. The extracellular matrix guides the orientation of the cell division axis. *Nat. Cell Biol.* 7:947–953.

Thery, M., V. Racine, M. Piel, A. Pepin, A. Dimitrov, Y. Chen, J.B. Sibarita, and M. Bornens. 2006. Anisotropy of cell adhesive microenvironment governs cell internal organization and orientation of polarity. *Proc. Natl. Acad. Sci. USA.* 103:19771–19776.

Vleminckx, K., L. Vakaet Jr., M. Mareel, W. Fiers, and F. van Roy. 1991. Genetic manipulation of E-cadherin expression by epithelial tumor cells reveals an invasion suppressor role. *Cell.* 66:107–119.